



# Grain growth in a nanostructured AZ31 Mg alloy containing second phase particles studied by phase field simulations

Yan Wu<sup>1\*</sup>, Yaping Zong<sup>2</sup> and Jianfeng Jin<sup>2</sup>

**ABSTRACT** Phase field models were established to simulate the grain growth of a nanostructured AZ31 magnesium alloy, which contain spherical particles of differing sizes and volume fractions, under realistic spatial and temporal scales. The effect of the second phase particles on the nanostructure evolution was studied. The simulated results were compared with those of the conventional microstructured alloy. The expression of the local free energy density was improved by adding a second phase particle term. The right input parameters were selected for proper physical meaning. It was shown that the rules that govern the pinning effect of the second phase particles during the grain growth were different for the nanostructure and microstructure. There was a critical particle size value that affected the grain growth within the nanostructure. If the particle size was lower than the critical value, the pinning effect on grain growth increased with decreasing particle size. When the particle size was greater than the critical value, the particles had almost no pinning effect. However, in the conventional microstructured material, the larger particle size resulted in an enhanced pinning effect during grain growth for particle sizes smaller than 1  $\mu\text{m}$ . The effect was reversed when the particle size was larger than the critical value. For the nanostructure, the critical value was 200 nm when the particle content was 10 v.%, and the critical value decreased when the content increased. When the particle size was 30 nm, the particle pinning effect on the grain growth increased for increasing particle content.

**Keywords:** phase field models, second phase particles, grain growth, magnesium alloy

## INTRODUCTION

Magnesium alloys are the lightest structural materials. They have received much attention in recent years due to their excellent properties [1–4]. They have been widely

used in automobiles, aerospace, 3C products and other industrial fields [5]. The AZ31 Mg alloy is a widely used commercial deformation magnesium alloy, and thus it is chosen as the base-line material in research. The solubility of Al and other elements in an Mg alloy is low, and thus the solution and aging strengthening are ineffective. Therefore, several methods were explored to improve the mechanical properties of the AZ31 alloy, including nanocrystallization and refining the grain size by introducing second phase particles.

Grain refining is an important strategy to improve the mechanical properties, such as the strength and toughness, through Hall-Petch relation in polycrystalline materials [6–8]. Finely dispersed hard particles are usually used to control the microstructure evolution in materials and obtain a smaller grain size, by pinning the grain boundaries and preventing grain growth. The second phase particles can be added during the material preparation process.

It is difficult to experimentally prepare a series of second phase particles, with different sizes and volume fractions. Computer simulation is a convenient way to investigate the influence of these particles on grain growth. Phase field methods, based on continuum diffusion equations, have been established to investigate the effect of second phase particles on the microstructure evolution [9–12]. Moelans *et al.* [9] presented a phase field model to simulate polycrystalline grain growth for grains that contain small incoherent second phase particles. They also studied the pinning effect on the microstructure evolution. Zhou *et al.* [11] investigated the effect of particles with different shapes, volume fractions and sizes on the grain growth of two different phases by phase field methods. Mallick [12] examined

<sup>1</sup> School of Mechanical Engineering, Wuhan Polytechnic University, Wuhan 430000, China

<sup>2</sup> Key Laboratory for Anisotropy and Texture of Materials (Ministry of Education), Northeastern University, Shenyang 110819, China

\* Corresponding author (email: [wuy611@163.com](mailto:wuy611@163.com))

the effect of mobile second phase particles on the kinetics of polycrystalline grain growth using a phase field theory. However, these models are not in real time and space, in contrast to actual alloys.

There are experimental reports of the effect of second phase particles on grain growth of Mg alloys [13,14]. On the other hand, our previous work has already achieved a phase field model to simulate the grain growth process of the AZ31 alloy in real time and space. The simulated results agreed well with those of experiments [15–18], which were achieved by introducing a new concept concerning the grain boundary range. It is believed that the models are the first to accomplish the simulation of grain growth and the evolution of the microstructure on a realistic spatiotemporal and industrial scale. However, as far as the authors know, no phase field model was reported for the nanoscale grain growth process containing second phase particles in a real alloy. Then, the grain growth in nanostructural AZ31 Mg alloy containing second phase particles has been studied by phase field method in this research.

In this study, phase field models were built to investigate the grain growth of a polycrystalline AZ31 Mg alloy, which contained second phase particles, with their size varying between nano- and micrometer scale, using a realistic spatio-temporal process. The previously used expression of the local free energy function was improved by introducing second phase particles to the expression. The effects of second phase particles of different sizes and volume fractions on the nanostructure and microstructure were examined, in order to find out the refinement mechanisms for this unique nanostructure and to establish a reference study for the development of nanocrystalline materials. This study aims to provide theoretical guidance for the introduction of second phase particles by compound addition or *in situ* reaction synthesis to the AZ31 alloy on the microstructural level.

## MODEL DESCRIPTION

The phase field methods are based on thermodynamic and kinetic equations. The temporal evolution of the microstructure can be determined by evaluating the time-dependent Allen-Cahn equation and Cahn-Hilliard diffusion equation as follows [19,20]:

$$\begin{aligned} \frac{\partial \eta_p(\mathbf{r}, t)}{\partial t} &= -L \frac{\delta F}{\delta \eta_p(\mathbf{r}, t)}, \quad (p = 1, 2, 3, \dots, n) \\ \frac{\partial c(\mathbf{r}, t)}{\partial t} &= M \nabla^2 \frac{\delta F}{\delta c(\mathbf{r}, t)}, \end{aligned} \quad (1)$$

where  $L$  and  $M$  are the structural relaxation and chemical

mobility parameters, respectively. The long-range orientation parameter,  $\eta_p(\mathbf{r}, t)$ , is used to distinguish the different orientation relationships of the grains. The concentration field is represented by  $c(\mathbf{r}, t)$ . The possible number of different grain orientations in the system,  $p$ , was set to 32, as suggested in reference [15].  $F$  is the free energy of the system and its expression in isotropic single-phase system is shown as follows [21]:

$$F = \int_V [f_0(c, \eta_1(\mathbf{r}, t), \eta_2(\mathbf{r}, t), \dots, \eta_p(\mathbf{r}, t)) + \frac{K_2}{2} \sum_{p=1}^n (\nabla \eta_p(\mathbf{r}, t))^2] d\mathbf{r}, \quad (2)$$

where  $K_2$  is the gradient energy coefficient and  $f_0$  is the local free energy density function.

When the second phase particles remain immobile and their shapes are unchanged throughout the evolution of the microstructure, the local free energy density generated by the second phase particles is expressed as  $f_0^p = \Phi \sum_{p=1}^n \eta_p^2$ , ( $p = 1, 2, \dots, n$ ) [9]. Here,  $\Phi$  is used to describe the particle distribution. When  $\Phi = 1$ , there is a particle, while when  $\Phi = 0$ , there are no particles, while  $\Phi$  is considered to be constant with time. The local free energy density of the system is described by the following expression:

$$\begin{aligned} f_0 &= A + A_1(c(\mathbf{r}, t) - c_1)^2 + \frac{A_2}{4}(c(\mathbf{r}, t) - c_1)^4 \\ &\quad - \frac{B_1}{2}(c(\mathbf{r}, t) - c_1)^2 \sum_{p=1}^n \eta_p^2(\mathbf{r}, t) + \frac{B_2}{4}(\sum_{p=1}^n \eta_p^2)^2 \\ &\quad + \frac{K_1}{2} \sum_{p=1}^n \sum_{p \neq q} \eta_p^2(\mathbf{r}, t) \eta_q^2(\mathbf{r}, t) \\ &\quad + \Phi \sum_{p=1}^n \eta_p^2, \end{aligned} \quad (3)$$

where  $c_1$  is the concentration at the lowest point of the free energy curve as a function of concentration at a certain temperature and  $K_1$  is the coupling coefficient of  $\eta_i$  and  $\eta_j$ . If  $\Phi = 0$ ,  $f_0$  becomes the minima when  $\eta_q^2 = 1$  and  $\sum_{p \neq q} \eta_p^2 = 0$ , while if  $\Phi = 1$ ,  $f_0$  becomes the minima when  $\sum_{p=1}^n \eta_p^2 = 0$ .

The AZ31 Mg alloy was selected for the model with an alloy composition of 96 wt.% Mg, 3 wt.% Al and 1 wt.% Zn. The temperature was set to 350°C, while the rest of the parameters in the model were determined by preliminary work that was performed for the present study, where  $c_1 = 0.2$ ,  $A = -25.01 \text{ kJ mol}^{-1}$ ,  $A_1 = 22.02 \text{ kJ mol}^{-1}$ ,  $A_2 = 18.30 \text{ kJ mol}^{-1}$ ,  $B_1 = 3.54 \text{ kJ mol}^{-1}$ ,  $B_2 = 92.86 \text{ kJ mol}^{-1}$ ,  $K_1 = 141.24 \text{ J mol}^{-1}$ ,  $K_2 = 35.37 \times 10^{-13} \text{ J m}^2 \text{ mol}^{-1}$  and  $L = 1.15 \times 10^{-2} \text{ mol J s}^{-1}$ , when referring to the microstructure [15]. Additionally,  $A = -25.57 \text{ kJ mol}^{-1}$ ,  $A_1 = 99.14 \text{ kJ mol}^{-1}$ ,  $A_2 = 18.30 \text{ kJ mol}^{-1}$ ,  $B_1 = 80.33 \text{ kJ mol}^{-1}$ ,  $B_2 = 2321.51 \text{ kJ mol}^{-1}$ ,

$K_1 = 2090.16 \text{ J mol}^{-1}$ ,  $K_2 = 0.21 \times 10^{-13} \text{ J m}^2 \text{ mol}^{-1}$  and  $L = 2.07 \times 10^{-6} \text{ mol J}^{-1} \text{ s}^{-1}$ , when referring to the nanostructure [16]. Each parameter has its own physical meaning, which is described in detail in the literature [15,16].

The nucleation process of crystallization is simplified by a phenomenological method and the well-defined microstructure is formed after a short period of time. The initial state is given as  $4dx \times 4dx$  grid units, evenly distributing in the simulated area, and the radius of the nucleus is a random value ranging between 0 and 2 grid units. The local initial composition is considered to be 0.03. The value of the time step has to be relatively small in order to obtain convergence in the results; however, an extremely small value for the time step requires more steps for solving the kinetic equations [22]. To balance the two factors, a time step of 0.6 s was selected for the nanoscale model and 0.3 s for the microscale model. The periodic boundary is defined as the boundary condition for the differential equations, in order to minimize the boundary effect on the grain growth kinetics.

## SIMULATION RESULTS

In this study, phase field models are used to investigate the morphology and evolution of the polycrystalline structure of the AZ31 Mg alloy. The actual and simulated morphologies are compared to validate the accuracy of the models. Traditional experimental methods can only observe

the morphology of the structure at a certain temperature and a certain time. It is difficult to observe the evolution of the polycrystalline structure as a function of annealing time, especially grain boundary movement and pinning by the second phase particles. However, the phase field models can track the continuously changing morphology of materials during a heat treatment. These models help researchers study the pinning effects of the second phase particles on the grain boundaries, and optimize the material properties.

### The effect of second phase particle sizes on the grain growth of the nanostructure

There are  $512 \times 512$  two-dimensional uniform grids in the nanoscale models. For the nanostructure, the overall size of the simulation cell is  $1.5 \mu\text{m} \times 1.5 \mu\text{m}$ . Each grid size of 2.93 nm and 10 v.% of second phase particles are defined during the nucleation in the nanostructure, with a particle diameter of 10, 20, 30, 100, 200 or 300 nm. The simulated results at 500 min and  $350^\circ\text{C}$  are presented in Fig. 1.

As shown in Fig. 1,  $\eta_p^2 = 1$  represents the grains whose orientation number is  $p$ , so the color is white in the gray image;  $\eta_p, \eta_q \in (0, 1)$  represent the grain boundary of the  $p$  grain and  $q$  grain, so the color is gray. The white grains are separated by the gray grain boundaries. The orientation value is 0 when it is located on the second phase particles, where the color is black. The morphology is consistence

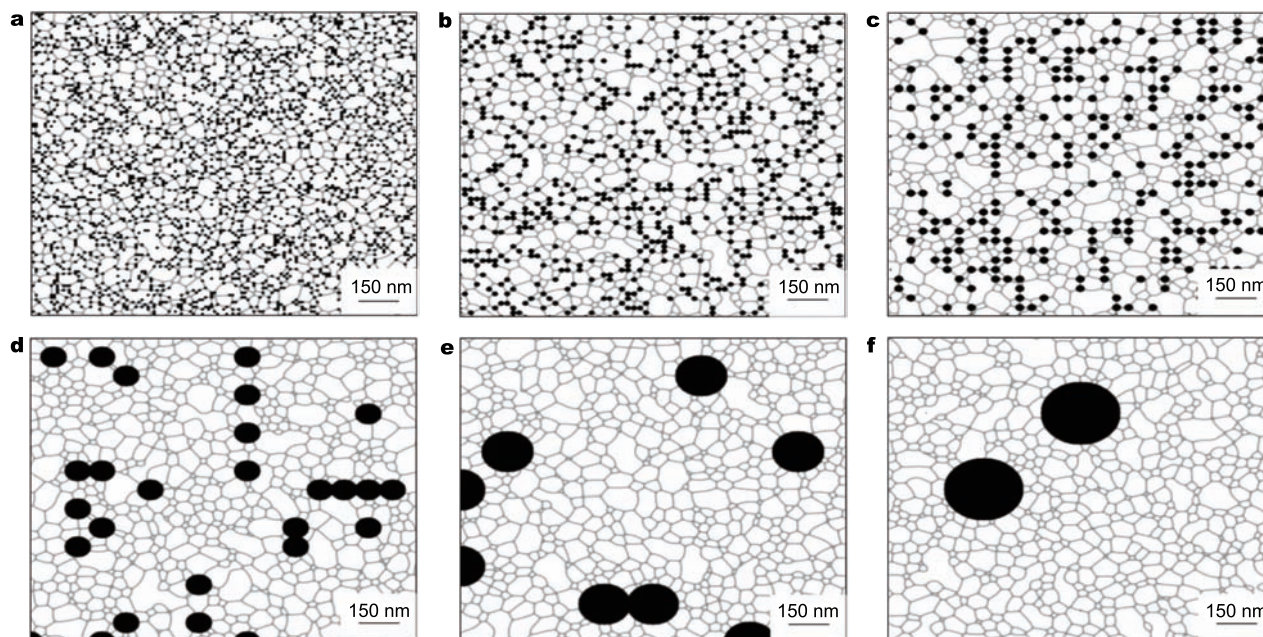


**Figure 1** Nanostructure containing 10 v.% second phase particles. Their sizes are 10, 20, 30, 100, 200 and 300 nm. When the annealing time is  $t = 500$  min at  $350^\circ\text{C}$ : (a)  $d = 10$  nm, (b)  $d = 20$  nm, (c)  $d = 30$  nm, (d)  $d = 100$  nm, (e)  $d = 200$  nm, (f)  $d = 300$  nm.

with that observed in traditional experiments.

Most of the particles are located at the grain boundaries, so parts of the grain boundary are replaced by particles, reducing the grain boundary energy. The driving force behind grain growth comes from the reduced free energy. However, the reduction in free energy is counter balanced by particle pinning. The larger the grain size, the stronger is the pinning effect.

The influence of particle size on the grain growth process was investigated for a 10 v.% particle fraction. The corresponding results are presented in Fig. 2.

As shown in Fig. 2, the average grain size increases with an increase during annealing. The average grain size decreases with a reduction in particle size for the same annealing time, for particle sizes of 10, 20, 30 or 100 nm. This effect is observed because the number of particles increases as the particle size decreases, for a constant volume fraction of particles. A single grain boundary may be pinned by more particles of a smaller size, inducing greater resistance for grain boundary movement and slowing the rate of grain growth. This phenomenon is consistent with the law of Zener pinning [23]. It is also observed that the grain size of a nanostructure that does not contain any particles is similar to the structure containing particles of 200 or 300 nm in diameter. Thus, a critical particle size of < 200 nm can influence grain growth in the nanostructure at a particle fraction of 10 v.%. If the particle size is lower than 200 nm, the pinning effect on grain growth increases by decreasing the particle size, while, if the size is higher than 200 nm, the particles have almost no pinning effect on the grain growth within the nanostructure.

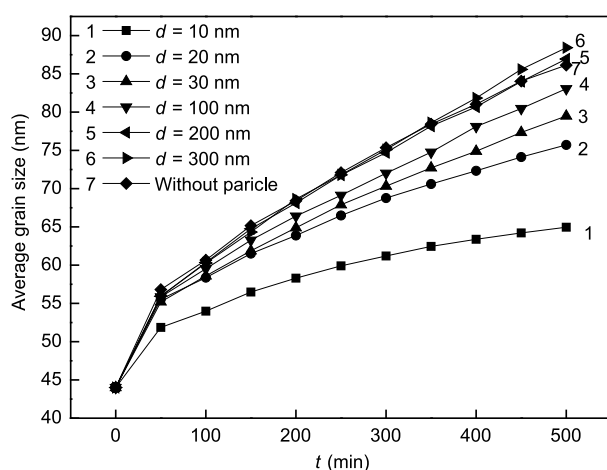


**Figure 2** The relationship of average grain size with annealing time in the nanostructure. The alloy contains 10 v.% of second phase particles of differing size at 350°C.

### The effect of second phase particle size on the grain growth of the microstructure

A fraction of 10 v.% of second phase particles was introduced into the microstructure. The particle sizes were 100, 200, 300 nm, 1, 2 and 3  $\mu\text{m}$ . When the size of the second phase particles was 1, 2 or 3  $\mu\text{m}$ , uniform two-dimensional grids of  $512 \times 512$  were selected for the micron models. The grid unit size was 0.293  $\mu\text{m}$  and the entire simulation area was  $150 \mu\text{m} \times 150 \mu\text{m}$ . However, when the size of the particles was 100, 200, or 300 nm, the initial state was changed, selecting a grid unit of 0.1  $\mu\text{m}$ , a total number of  $1024 \times 1024$  grids and a unit time of 0.075 s. The other parameters were left unchanged from those described in Ref. [7]. The simulated results at 100 min are presented in Fig. 3.

As shown in Fig. 3, when the second phase particle size is 100, 200 or 300 nm, most of the particles are within the grains. The reason may be that the pinning effect of the sub-micrometer sized particles is too weak to impede the movement of the microscale boundaries. It can also be observed that when the size of the particles is 1, 2 or 3  $\mu\text{m}$ , most of the grain boundaries occur as straight lines in the microstructure after 100 min. If the curvature of the grain boundary is reduced, the driving force for grain growth will be decreased, and grains grow more slowly. On the other hand, most of the grain boundaries are presented as bent lines when they contain sub-micrometer sized particles. This means that the pinning effect on the microstructure of the microscale particles is stronger than that of the sub-micron particles. Larger particles allow the grains to reach a steady state more quickly.

The change in average grain size with respect to the annealing time for a microstructure containing 10 v.% of second phase particles, was quantitatively analyzed, and the results are presented in Fig. 4.

As shown in Fig. 4, for a 10 v.% fraction of particles in the microstructure, the grain growth rate is higher at the early stages, almost stopping completely at the later stages. When there are no particles in the microstructure, the grain size increases with increasing annealing time. The grain size increases with decreasing particle size for particles of 100, 200 or 300 nm, when keeping annealing time constant. This means that larger sub-micron particles induce stronger resistance to grain growth. This could be attributed to the fact that, for the microstructure, the sub-micron particles are too small to pin the microscale boundaries, but an incremental change in particle size may increase the pinning force on the grain boundaries. For particle sizes of 1, 2 or 3  $\mu\text{m}$ , the grain size increases with increasing particle size, keeping annealing time constant.

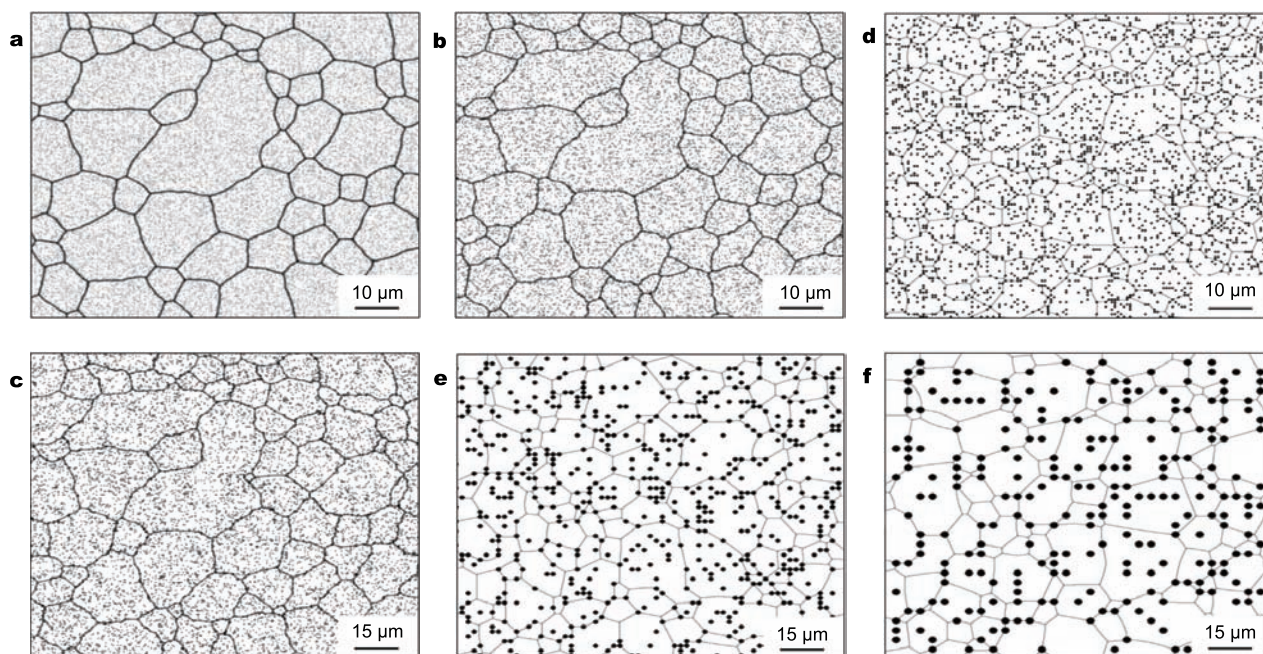


**Figure 3** Microstructure with 10 v.% second phase particles, with sizes of 100, 200, 300 nm, 1, 2 or 3  $\mu\text{m}$  and the annealing time is 100 min, at a temperature of 350°C: (a)  $d = 100$  nm, (b)  $d = 200$  nm, (c)  $d = 300$  nm, (d)  $d = 1$   $\mu\text{m}$ , (e)  $d = 2$   $\mu\text{m}$ , (f)  $d = 3$   $\mu\text{m}$ .

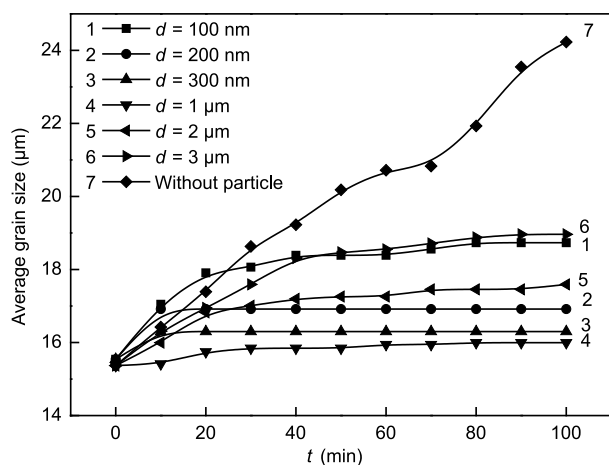


**Figure 4** Relationship between the average grain size and annealing time, for a microstructure containing 10 v.% of second phase particles at 350°C.

This is consistent with the law of Zener pinning and also with the calculations of nanoparticle-containing nanostructures. From Fig. 4, it can be observed that there is also a critical particle size of 1  $\mu\text{m}$  that affects the grain growth in the microstructure, for particle volume fractions of 10 v.%. If the particle size is less than 1  $\mu\text{m}$ , the grain size will increase with decreasing particle size, while, if the particle size is greater than 1  $\mu\text{m}$ , the grain size will increase with increasing particle size.

### The effect of volume fraction of second phase particles on the grain growth of the nanostructure

The simulated results presented in Fig. 5 correspond to a volume fraction in the nanostructure of second phase particles of 5 v.% and 15 v.% and a particle size of 30 nm.

In the model, the particles are spherically shaped; they are shown as round in the two-dimensional condition. As shown in Fig. 5, the shape and position of the second phase particles were unchanged, and most of the particles are located in the grain boundaries, especially at the trigeminal junction boundaries. The reason for this phenomenon is generally considered to be that when the particles are located on the grain boundaries, part of the grain boundary will be replaced by particles. This reduces the grain boundary energy and in turn reduces the total free energy of the system. This phenomenon is consistent with the physical law of grain growth evolution.

Further analysis of the changes in the average grain size as a function of annealing time was performed for particle volume fraction values of 0 v.%, 5 v.%, 10 v.% and 15 v.%. The particle size within the nanostructure was kept constant at 30 nm, at an annealing temperature of 350°C. The results are presented in Fig. 6.

As presented in Fig. 6, when the particle volume fraction is 0 v.%, 5 v.%, 10 v.% or 15 v.%, the grains coarsen with increasing annealing time. The average grain size values

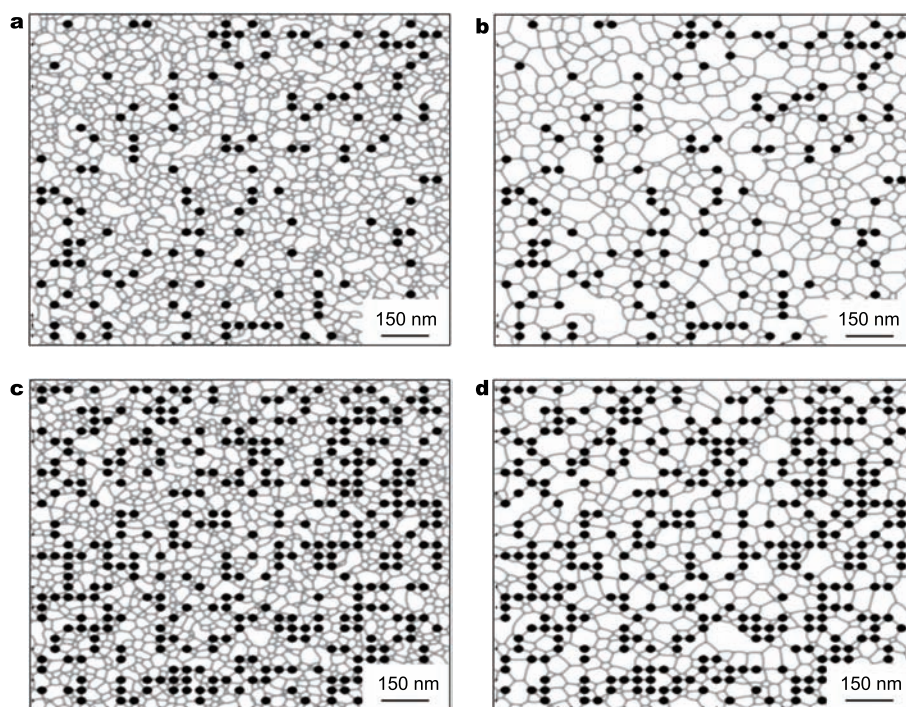


**Figure 5** Evolution in the nanostructure of the AZ31 Mg alloy, containing 5 v.% or 15 v.% particles, where the particle size is 30 nm: (a)  $t = 50$  min at 5 v.% particles, (b)  $t = 50$  min at 15 v.% particles, (c)  $t = 500$  min at 5 v.% of particles, (d)  $t = 500$  min at 15 v.% particles, at an annealing temperature of 350°C.

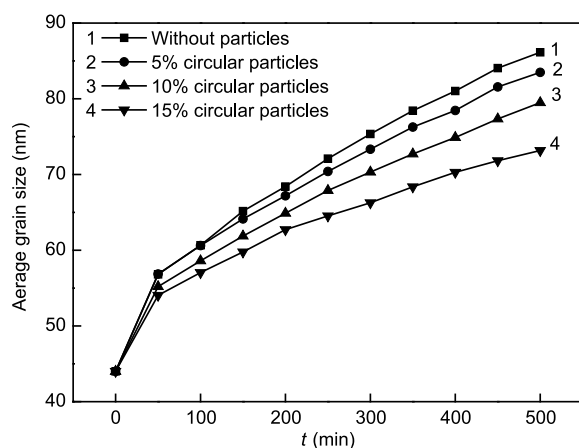


**Figure 6** The relationship between the average grain size and annealing time for particle volume fractions of 0 v.%, 5 v.%, 10 v.% or 15 v.%. The particle size is 30 nm within the nanostructure and the annealing temperature is 350°C.

for different volume fractions are similar. At the early stages of grain growth, and as the annealing time increases, the average grain size values decrease with increasing particle volume fraction. This means that a higher volume fraction of second phase particles will result in a stronger pinning effect, with the grains coarsening at lower rates,

which is consistent with the law of Zener pinning. The reason for this phenomenon may be that for larger volume fractions of particles, more particles will be located at the grain boundaries. Thus, the free energy of the system will be lower for larger volume fractions, and the system will be more stable, slowing the rate of grain growth. The change in the critical size of the second phase particles was studied by phase field simulation for a 15 v.% fraction of the second phase particles. The relationship between the average grain size and annealing time is presented in Fig. 7. The critical size of the second phase particles was also investigated and presented in Fig. 7.

As presented in Fig. 7, when the particle diameter is 10, 20 or 30 nm, the average grain size increases with increasing particle size for a 15 v.% fraction of the second phase particles. When the particle diameter is 100, 200 or 300 nm, the average grain size remains similar at a constant annealing time. These values are similar to that of the structure without particles, which means that there may be a critical size of the second phase particles for the 15 v.% fraction, and the value is different to that of the 10 v.% fraction. If the particle size diameter is lower than a critical size, smaller particles will result in a stronger pinning effect, while, if the particle size diameter is higher than this critical size,

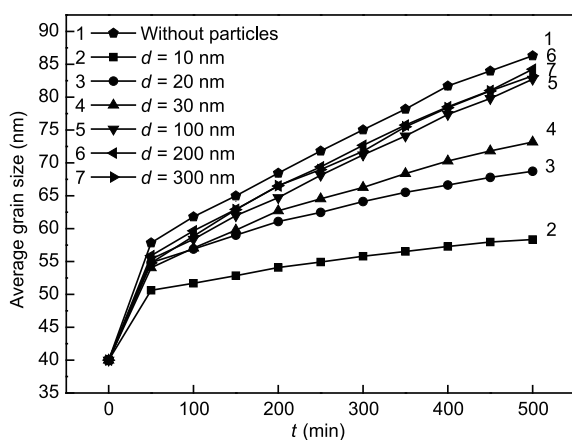


**Figure 7** Relationship between the average grain size and annealing time, at 15 v.% fraction of the second phase particles, using various radii within the nanostructure and an annealing temperature of 350°C.

the particles have almost no pinning effect.

## CONCLUSIONS

In this work, we established the phase field models to simulate the grain growth of nanostructured AZ31 Mg alloy, which was containing spherical particles under realistic spatial-temporal scales. It was found that the rule of pinning effect of the second phase particles during grain growth is different in the nanostructure from that in the conventional microstructure. Simulated results show there is a critical value of particle size that affects the grain growth in the nanostructure. If the particle size is lower than the critical value, the effect of pinning on grain growth will increase with decreasing size. If the particle size is higher than the critical value, the particles have almost no pinning effect. The simulation results show that there is also a critical particle size for the microstructure. If the particle size is lower than a critical value of 1  $\mu\text{m}$ , the pinning effect on grain growth will increase with increasing size, while the effect is reversed if the particle size is higher than the critical value. It was found that when the volume fraction of particles is increased from 0 to 15 v.%, the pinning effect of the particles on the grain growth also increases. The critical particle value is 200 nm, when the fraction of particles is 10 v.%, and the critical size decreases when the fraction is increased to 15 v.% in the nanostructure of the polycrystalline materials. The simulation results obtained will be very valuable to understand the mechanisms and laws of effect of second phase particles on the grain growth, and accurately control the introduction of second phase particles and material properties.

Received 17 March 2016; accepted 12 May 2016;  
published online 30 May 2016

- Lukyanova EA, Martynenko NS, Shakhova I, *et al.* Strengthening of age-hardenable WE43 magnesium alloy processed by high pressure torsion. *Mater Lett*, 2016, 170: 5–9
- Jiang L, Zhang D, Fang X, *et al.* The effect of Sn addition on aging behavior and mechanical properties of wrought AZ80 magnesium alloy. *J Alloys and Comps*, 2015, 620: 368–375
- Ray AS, Wilkinson DS. The effect of microstructure on damage and fracture in AZ31B and ZEK100 magnesium alloys. *Mater Sci Eng A*, 2016, 658: 33–41
- Radi Y, Mahmudi R. Effect of  $\text{Al}_2\text{O}_3$  nano-particles on the microstructural stability of AZ31 Mg alloy after equal channel angular pressing. *Mater Sci Eng A*, 2010, 527: 2764–2771
- Mordike BL, Ebert T. Magnesium: properties-applications-potential. *Mater Sci Eng A*, 2001, 302: 37–45
- Ali Y, Qiu D, Jiang B, *et al.* Current research progress in grain refinement of cast magnesium alloys: a review article. *J Alloys and Compd*, 2015, 619: 639–651
- Svyetlichnyy DS. Modeling of grain refinement by cellular automata. *Comput Mater Sci*, 2013, 77: 408–416
- Mallick A, Vedantam S, Lu L. Grain size dependent tensile behavior of Mg-3% Al alloy at elevated temperature. *Mater Sci Eng A*, 2009, 512: 14–18
- Moelans N, Blanpain B, Wollants P. Phase field simulations of grain growth in two-dimensional systems containing finely dispersed second-phase particles. *Acta Mater*, 2006, 54: 1175–1184
- Long YQ, Liu P, Liu Y, *et al.* Simulation of recrystallization grain growth during re-aging process in the Cu-Ni-Si alloy based on phase field model. *Mater Lett*, 2008, 62: 3039–3042
- Zhou GZ, Wang YX, Chen Z. Phase-field method simulation of the effect of hard particles with different shapes on two-phase grain growth. *Acta Metall Sin*, 2012, 48: 227–234
- Mallick A. Effect of second phase mobile particles on polycrystalline grain growth: a phase-field approach. *Comput Mater Sci*, 2013, 67: 27–34
- Radi Y, Mahmudi R. Effect of  $\text{Al}_2\text{O}_3$  nano-particles on the microstructural stability of AZ31 Mg alloy after equal channel angular pressing. *Mater Sci Eng A*, 2010, 527: 2764–2771
- Wang K, Chang L, Wang Y, *et al.* Preparation of Mg-AZ31 based composites with Ti particles by friction stir processing. *Chin J Non-ferrous Met*, 2009, 19: 418–423
- Zong YP, Wang MT, Guo W. Phase field simulation on recrystallization and secondary phase precipitation under strain field. *Acta Phys Sin*, 2009, 58: S161–S168
- Wu Y, Zong BY, Zhang XG, *et al.* Grain growth in multiple scales of polycrystalline AZ31 magnesium alloy by phase field simulation. *Metall Mater Trans A*, 2013, 44: 1599–1610
- Wu Y, Zong Y, Zhang X. Microstructure evolution of nanocrystalline AZ31 magnesium alloy by phase field simulation. *Acta Metall Sin*, 2013, 49: 789–796
- Zhang XG, Zong YP, Wu Y. A model for release of stored energy and microstructure evolution during recrystallization by phase field simulation. *Acta Phys Sin*, 2012, 61: 088104
- Allen SM, Cahn JW. A microscopic theory for antiphase boundary motion and its application to antiphase domain coarsening. *Acta Metall*, 1979, 27: 1085–1095
- Cahn JW, Hilliard JE. Free energy of a nonuniform system. I. Interfacial free energy. *J Chem Phys*, 1958, 28: 258–267
- Zhang XG, Zong YP, Wang MT, *et al.* A physical model to express grain boundaries in grain growth simulation by phase-field method.

*Acta Phys Sin*, 2011, 60: 068201

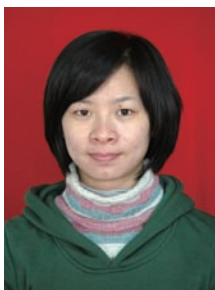
- 22 Wen YH, Wang B, Simmons JP, *et al.* A phase-field model for heat treatment applications in Ni-based alloys. *Acta Mater*, 2006, 54: 2087–2099
- 23 Humpherys FJ, Ardakani MG. Grain boundary migration and Zener pinning in particle-containing copper crystals. *Acta Mater*, 1996, 44: 2717–2727

**Acknowledgments** This work was supported by the National Natural

Science Foundation of China (U1302272).

**Author contributions** Zong Y conceived the study. Wu Y contributed analysis and manuscript preparation, data analyses and wrote the manuscript, Jin J helped perform the analysis with constructive discussions.

**Conflict of interest** The authors declare that they have no conflict of interest.



**Yan Wu** received her PhD degree from Northeastern University in 2014. Her research interests include studying the evolution of microstructures by phase field simulation and optimal microstructure design. She developed multiple scales of phase field models for grain growth in the AZ31 Mg alloy.

## 相场法对含第二相颗粒的纳米结构AZ31镁合金晶粒生长的模拟研究

吴艳<sup>1\*</sup>, 宗亚平<sup>2</sup>, 金剑锋<sup>2</sup>

**摘要** 本文建立了一个真实时空的相场模型模拟,研究了含不同尺寸和体积分数的球形第二相颗粒的纳米结构AZ31镁合金的晶粒生长过程;第二相颗粒对单相合金系统晶粒组织演化和生长动力学的影响;并将模拟结果与微米晶结构镁合金的模拟结果相比较.通过在自由能密度函数的表达式中增加第二相颗粒的表达来改进模型.模拟结果表明:纳米晶组织中第二相粒子对晶粒长大的钉扎作用,与对微米晶组织下的作用有很大区别.纳米结构中,第二相颗粒对晶粒长大影响存在一个粒子尺寸的临界值,当第二相颗粒体积分数为10%时,粒子尺寸的临界值为200 nm,随粒子含量增加,临界尺寸值将减小.另一方面,粒子含量越大对晶界钉扎作用越大,晶粒平均尺寸越小.该研究将为选择复合加入和原位合成的方法在AZ31镁合金中引入第二相颗粒的实验研究提供显微组织设计的理论指导.